Journal of Power Sources 196 (2011) 8057–8063

Journal of Power Sources

journal homepage: www.elsevier.com/locate/jpowsour

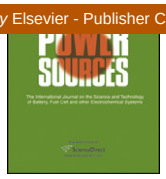

Magnesium oxide prepared via metal–chitosan complexation method: Application as catalyst for transesterification of soybean oil and catalyst deactivation studies

Gizelle I. Almerindo[a], Luiz F.D. Probst[a], Carlos E.M. Campos[b], Rusiene M. de Almeida[c,*], Simoni M.P. Meneghetti[c], Mario R. Meneghetti[c], Jean-Marc Clacens[d], Humberto V. Fajardo[e]

[a] Departamento de Química, Universidade Federal de Santa Catarina, 88040-900, Florianópolis – SC, Brazil
[b] Departamento de Física, Universidade Federal de Santa Catarina, 88040-900, Florianópolis – SC, Brazil
[c] Instituto de Química e Biotecnologia, Universidade Federal de Alagoas, 5702-970, Maceió – AL, Brazil
[d] Laboratoire de Catalyse en Chimie Organique (LACCO), Université de Poitiers, UMR CNRS 6503, 40 Avenue du Recteur Pineau, 86022 Poitiers Cedex, France
[e] Departamento de Química, Universidade Federal de Ouro Preto, 35400-000, Ouro Preto – MG, Brazil

ARTICLE INFO

Article history:
Received 17 March 2011
Received in revised form 5 May 2011
Accepted 12 May 2011
Available online 19 May 2011

Keywords:
Magnesium oxide
Chitosan
Ethanol
Biodiesel

ABSTRACT

A simple method to prepare magnesium oxide catalysts for biodiesel production by transesterification reaction of soybean oil with ethanol is proposed. The method was developed using a metal–chitosan complex. Compared to the commercial oxide, the proposed catalysts displayed higher surface area and basicity values, leading to higher yield in terms of fatty acid ethyl esters (biodiesel). The deactivation of the catalyst due to contact with CO_2 and H_2O present in the ambient air was verified. It was confirmed that the active catalytic site is a hydrogenocarbonate adsorption site.

1. Introduction

Magnesium oxide (MgO) is a potential catalyst for various reactions due to the unique basic character of its surface, as demonstrated by an isoelectric point of around 12 [1–7]. For this reason MgO can catalyze the transesterification reactions of vegetable oils to biodiesel with short-chain alcohols. Being a heterogeneous catalyst, MgO could improve the synthesis methods by eliminating the additional costs associated with conventionally used homogeneous catalysts [8–12]. In this regard, the heterogeneous catalysts are economically and ecologically important when compared with homogeneous catalysts because they are environmentally benign, much easier to separate from liquid products, they facilitate the purification stages, can be reused, are non-corrosive, have high thermal stability and present fewer disposal problems [11].

Many types of heterogeneous catalysts for the production of biodiesel can be found in the literature, for example, alkaline earth oxides and several alkaline metal compounds supported on alumina or zeolite [11]. Many of these catalysts have high efficiency and activity in the transesterification reaction, however, under conditions of high temperature and pressure, and with long reaction times.

Therefore, it is of interest to investigate the possibility of replacing the homogeneous base catalysts by solid base catalysts in transesterification reactions associated with lower temperatures and shorter reaction times than those normally found in the literature for heterogeneous catalysts. In the literature, high methyl ester yields with the use of heterogeneous catalysts are also associated with the reaction occurring at high temperatures (170–250 °C) and with longer reaction times, in a continuous or batch reactor [8]. However, published study showed that nanocrystalline MgO catalysts can be used effectively as heterogeneous catalysts in the methylic transesterification of vegetable oils at low temperatures [1].

Another important factor is the possibility to store the catalysts and guarantee their catalytic activity for immediate use. However, base catalysts can lose their activity on contact with ambient air due to the adsorption of CO_2 and H_2O at the surface of the solid as carbonates and hydroxyl groups [13]. Granados et al. [14] investigated the effect of CO_2 in air on the activity of CaO in the transesterification of sunflower oil. This CaO catalyst gradually lost its activity because its surface sites were poisoned by contact with CO_2 and H_2O in air. However, the effects of H_2O and CO_2 on the catalytic

* Corresponding author. Tel.: +55 82 3214 1773; fax: +55 82 3214 1384.
E-mail address: rusiene@hotmail.com (R.M. de Almeida).

0378-7753
doi:10.1016/j.jpowsour.2011.05.030

properties of base catalysts and the deactivation mechanism have not been fully investigated [15].

More specifically, short chain alcohols (methanol or ethanol) are normally used in the production of biodiesel, however, few studies involving heterogeneous catalysis in the production of ethylic biodiesel are found in the literature [16]. Ethanol has several advantages compared to methanol, which is generally obtained from raw materials of fossil origin, with low toxicity, producing biodiesel with a greater cetane index and with greater lubricity, but the most important is probably its renewable origin [17–19]. However, ethanol is less reactive, requiring a greater excess of this alcohol to obtain yields similar to those obtained with methanol. Furthermore, longer reaction times are required, higher temperatures, anhydride alcohol, and oil with low water content for the separation of glycerol [20].

The objective of this study was to prepare MgO catalysts for the transesterification reaction of soybean oil with ethanol for the production of biodiesel. In this paper we verified the potential of MgO as a transesterification catalyst, prepared using a metal–chitosan complexation method, and compared it to that of a commercial magnesium oxide. The deactivation of the catalyst prepared using the method here proposed due to contact with the CO_2 and H_2O present in ambient air was also verified.

2. Experimental

2.1. Sample preparation and characterization

For the MgO extrudate preparation, 15.3 g of chitosan (Aldrich) were dissolved in 300 mL of CH_3COOH solution (10%, v/v) and 31.8 g of $Mg(NO_3)_2{\cdot}6H_2O$ (Vetec) were dissolved in distilled water. An aqueous solution of magnesium salt (Mg) was then added to the polymer solution under stirring. The chitosan monomer to Mg molar ratio was 1.5–2.0. The Mg–chitosan solution was added to a NH_4OH solution (50%, v/v) under vigorous stirring, in the form of extrudates, with a peristaltic pump. The gel extrudates formed were removed from the NH_4OH solution and dried at ambient temperature for 120 h. The MgO sample was obtained by calcining the dried samples at 550 °C in airflow for 4 h with a heating rate of 5 °C min^{-1}.

In this context, the MgO prepared as described above was compared with commercial MgO obtained from Riedel-de Haën (99.9% purity). These were designated as fresh catalysts, since the catalytic test was carried out immediately after calcination. In order to verify the effect of storage on the deactivation of the catalyst obtained using the method described above, it was exposed for a period of 180 days in ambient air to extend the carbonation and hydration processes. This catalyst was called MgO(stored).

Infrared spectra were obtained from 400 to 4000 cm^{-1}; the samples (2 mg dried chitosan and Mg–chitosan samples) were mechanically blended with 200 mg of KBr. The data were recorded using an FT Perkin-Elmer 16 PC infrared spectrophotometer.

The thermogravimetric analysis (TGA) was performed with a Shimadzu TGA-50 thermobalance using 11 mg of sample (Mg–chitosan) with a heating rate of 10 °C min^{-1} and airflow of 50 mL min^{-1}.

Samples were characterized by N_2 adsorption/desorption isotherms obtained at the temperature of liquid nitrogen using an automated physisorption instrument (Autosorb-1C, Quantachrome Instruments). Prior to the measurements, the samples were outgassed in a vacuum at 200 °C for 2 h. Specific surface areas were calculated according to the Brunauer–Emmett–Teller (BET) method, and the pore size distributions were obtained according to the Barret–Joyner–Halenda (BJH) method from the adsorption data.

Temperature programmed desorption (TPD) of CO_2 measurements were performed using a Quantachrome ChemBET 3000.

The crystalline structure of the dried powder sample was determined by X-ray diffraction (XRD) with a PanAnalytical diffractometer (Xpert PRO model) using Cu Kα (λ = 1.5418 Å) as the incident radiation, operating at 40 kV and 30 mA. To better define the structural parameters obtained from the XRD pattern a Rietveld analysis procedure was performed using the GSAS software program and a starting model based on information given on the ICSD card number 52026 [21–23]. The average crystallite size and microstrain were calculated by subtracting the instrumental line broadening contribution using the yttrium oxide standard and the formalism presented by Larson and Von Dreele [21].

The sample morphology was observed on scanning electron micrographs, obtained with a Philips XL30 scanning electron microscope operating at an accelerating voltage of 20 kV.

Thermogravimetric analysis coupled with mass spectrometry (TG-MS) were performed on a SDT Q600 apparatus from TA Insruments coupled by a heated capillary column with a Prisma QMS 200 mass spectrometer from Balzers. To measure the amount of CO_2 (m/z = 44) and H_2O (m/z = 18) formed, the samples were heated to 900 °C (heating rate: 10 °C min^{-1}) under a dried air (100 mL min^{-1}).

2.2. Catalytic test – transesterification experiments

All transesterification reactions were carried out in a 250 mL closed batch reactor equipped with a temperature-controlled bath, reflux condenser and a magnetic stirrer operating at 1000 rpm. The reactions were normally performed at 150 °C during 3 h with ethanol:oil:catalyst molar ratio of 600:100:5. Soybean oil (commercial grade) was supplied by Bunge Alimentos S.A and was used as received. After of reaction, the reaction mixture was washed three times with distilled water and centrifuged at 5000 rpm for 10 min.

In order to quantitatively evaluate the leaching of solid base catalyst under the reacting condition, fatty acid ethyl esters fraction was sent for elemental analysis via flame atomic absorption analysis (FLLA).

2.3. Analytical procedures

The fatty acid ethyl esters (FAEEs) obtained from the transesterification reaction were determined by gas chromatography using a Varian 3400 CX instrument, equipped with a capillary injection system operating at 240 °C, with a split ratio of 100:1 and sample size of 1 μL. An apolar capillary column VF-1ms (Factor Four), with 2.2 m length, 0.32 mm internal diameter and 0.1 mm film thickness, was employed and the column temperature program was: initial temperature of 50 °C (1 min), 15 °C min^{-1} to 180 °C, 7 °C min^{-1} to 230 °C and 30 °C min^{-1} to 245 °C. The detection system was equipped with a flame ionization detector (FID) operating at 250 °C. The carrier gas was high purity hydrogen.

The yield (%FAEEs) was quantified in the presence of tricaprylin as the internal standard. Approximately 0.15 g of the products obtained using the transesterification procedure described in Section 2 was weighed in a vial. An amount of 1 mL of tricaprylin solution (0.01 g/100 mL hexane) was added. This solution was injected into the chromatographic apparatus and the peak areas of the compounds were integrated.

Each experiment was run twice and the value obtained for each sample was the average of two injections. The biodiesel yield (%FAEEs) was calculated as in the Eq. (1).

$$\%\text{FAEEs} = \frac{m_{\text{tricaprylin}}\ A_B f_{\text{tricaprylin}}}{A_{\text{tricaprylin}}\ m_s} \quad (1)$$

where, $m_{tricaprylin}$ is the weight of the internal standard, A_B the peak area of FAEEs, $f_{tricaprylin}$ the response factor, $A_{tricaprylin}$ the peak area of the internal standard, and m_s the sample weight.

The free fatty acids found in the soybean oil (characterized as oleic acid, in the percentages given in the AOCS official method Ca 5a-40) totaled 0.1%.

3. Results and discussion

3.1. Sample characterization

The infrared spectra for chitosan (Cht) and the Mg–chitosan composite (Mg–Cht) taken before the calcination process (Fig. 1) were analysed in order to obtain information on the functional groups that participate in the binding or interaction with Mg in the intermediate stage of the porous MgO extrudate preparation.

In polymeric associations hydroxyl groups absorb in the form of a broad band at around 3400 cm^{-1} [24]. The bands in the region of 3440 cm^{-1} in the two spectra are associated with stretching of the OH groups overlapped with N–H stretching of the chitosan biopolymer. There was no displacement in relation to the wavenumber indicating that the intermolecular interactions, by way of the biopolymer hydrogen bonds, were maintained. The decrease in the intensity of the band in 3440 cm^{-1} on the spectrum for the compound (Mg–chitosan) is due to the interaction of Mg with the oxygen atoms of the hydroxyl groups as well as of the amine groups of the biopolymer bound to the glycoside ring. In addition, bands at 1650 and 1600 cm^{-1} on the chitosan spectrum were, respectively, associated with the C=O stretching vibration of secondary amide groups from the partially deacetylated chitin residues and with the N–H deformation vibrations of the primary amines of chitosan [25]. The reduction of these bands of the Mg–chitosan complex is related to the interaction of Mg with carbonyl groups from the partially deacetylated chitin residues as well as the interaction of the manganese ion with amine groups. Due to the incomplete deacetylation of chitosan (90%) mentioned previously the band at 1380 cm^{-1}, which is attributed to the C–H deformation of the CH_3 group, is associated with the few remaining acetamide groups present in the polymeric chain [25]. It can thus be noted that the amine groups of chitosan are the main effective bonding sites for the metallic ions, resulting in complexes stabilized by coordination. Nitrogen electrons present in the amine and N-acetylamine groups can establish coordinate covalent bonds with metal ions and some hydroxyl groups present in chitosan can act as donors [26]. The infrared spectra (IR) confirm the modification of certain characteristic regions of the functional groups of the biopolymer, mainly those which are susceptible to interaction with the Mg salt, without modifying the semicrystalline chitosan structure.

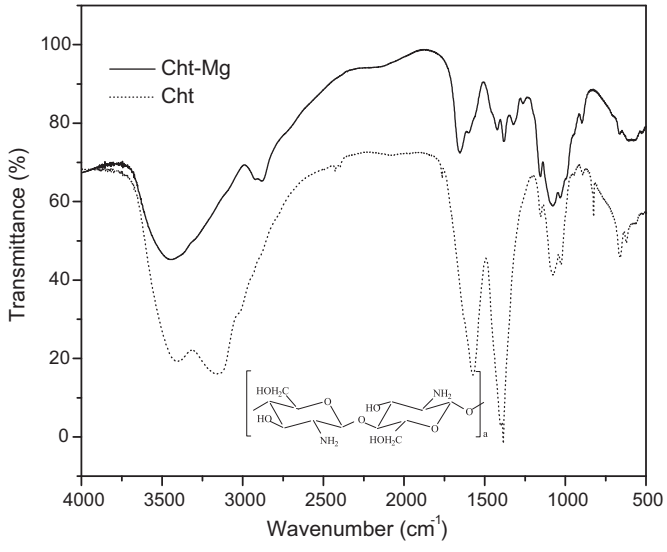

Fig. 1. Infrared spectra of chitosan (Cht) and chitosan–Mg (Mg–Cht) composite before heat-treatment process. Inset: chemical structure of chitosan.

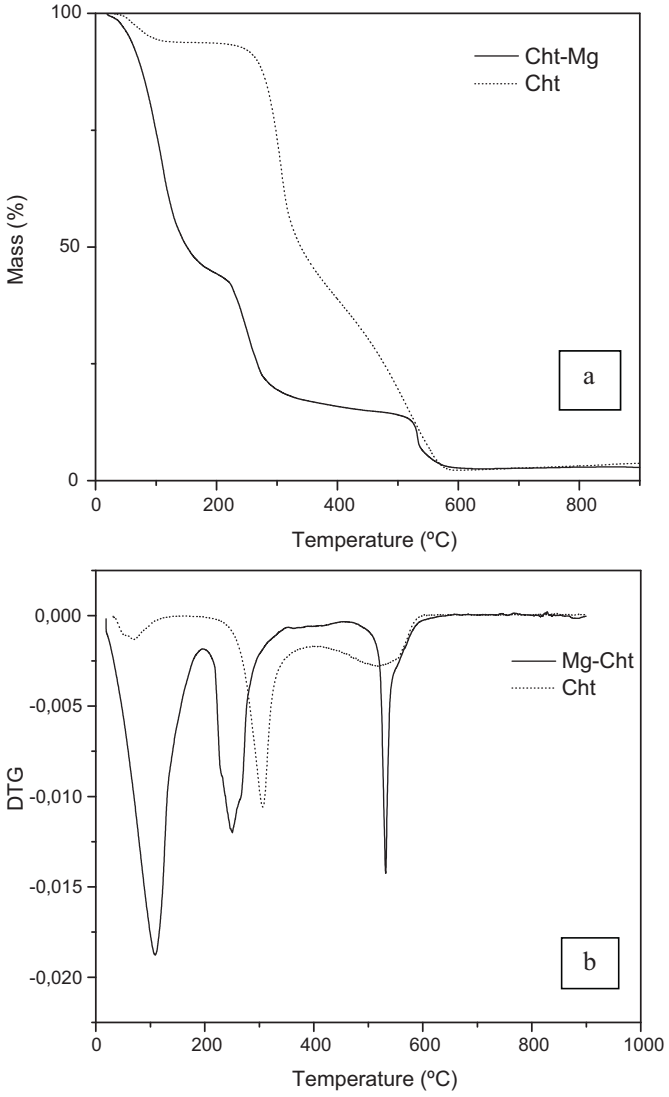

Fig. 2. Thermogravimetric analysis of chitosan (Cht) and chitosan–Mg (Cht–Mg).

The thermogravimetric (TGA/DTG) profiles are show in Fig. 2a and b. It can be seen that the elimination of residual material is dependent on the sample composition (chitosan or Mg–chitosan composite). The presence of magnesium leads to the removal of carbonaceous materials at lower temperatures. The TGA profile suggests a temperature of 550 °C for the total elimination of the residual material of the Mg–chitosan compound and 580 °C for the pure chitosan. The TGA and IR results confirm the formation of a novel material.

As summarized in Table 1, the preparation method led to a sample with better textural properties, such as specific surface area and pore volume, than the commercial sample (MgO(C)). Thus, the biopolymer must be used with the precursor material, which is eliminated during the thermal treatment generating the pores (215 Å) that contribute to the observed increase in surface area [27]. The surface area and pore volume are considered to be important parameters affecting the overall performance of a catalyst.

Table 1
Texture parameters calculated from N_2 adsorption isotherms and catalytic performances at ethanol:oil:catalyst molar ratio of 600:100:5, at 150 °C/3 h.

Catalyst	S_{BET} ($m^2\ g^{-1}$)	V_{BJH} ($cm^3\ g^{-1}$)	%FAEEs
MgO*	54.4	0.292	75
MgO(C)*	14.2	0.024	30
MgO(stored)	40	0.250	14

S_{BET} = specific surface area; V_{BHJ} = pore volume; MgO(C) = commercial oxide; %FAEEs = biodiesel yield.
* Fresh catalysts.

The XRD pattern of the fresh MgO powder (Fig. 3) shows very strong, slightly broadened peaks, consistent with nanometric-sized *fcc* MgO crystals (space group *Fm*-3*m*) with lattice parameters (4.22203 Å). The average size and microstrain of the MgO crystallites were 150 Å and 1.4%, respectively.

Scanning electron microscopy (SEM) was carried out in order to observe the morphologies of the samples obtained (MgO fresh). The SEM image shown in Fig. 4 reveals that the sample prepared using the method here developed has a porous aspect, consistent with the higher values for specific surface area and pore volume obtained from the physical measurement of N_2. During the calcination step the elimination of volatile materials occurs, and cavities are produced as a result of their removal. At the same time, a solid rearrangement takes place, forming the crystalline matrix. However, the sample stored for a period of 180 days in ambient air does not show the same aspect, as shown in Fig. 5, possibly due to the chemisorption of CO_2 and H_2O at the surface sites as hydrogenocarbonate species.

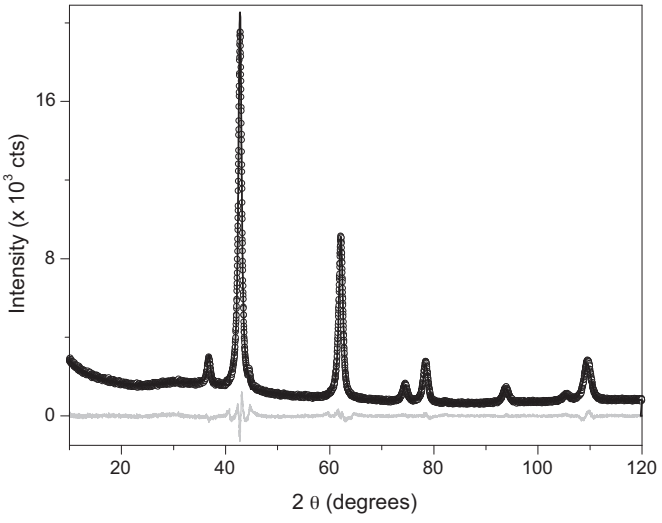

Fig. 3. XRD: experimental (noisy line) and calculated (thick line) XRD patterns of fresh MgO sample produced by metal–chitosan complexation method. Grey line represents the difference between experimental and calculated patterns.

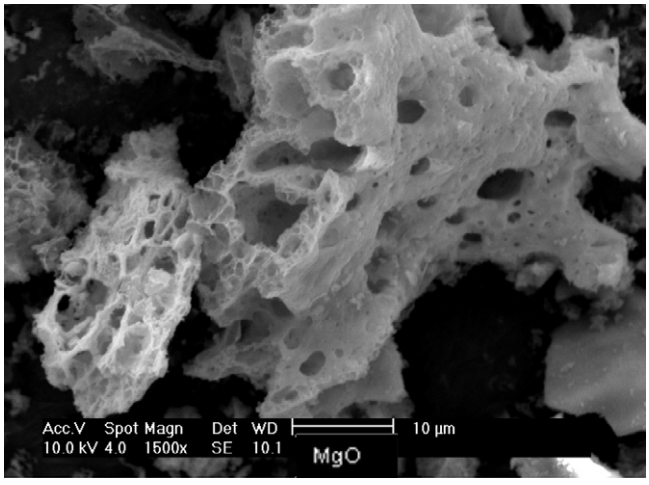

Fig. 4. Scanning electron microscopy (SEM) image of MgO.

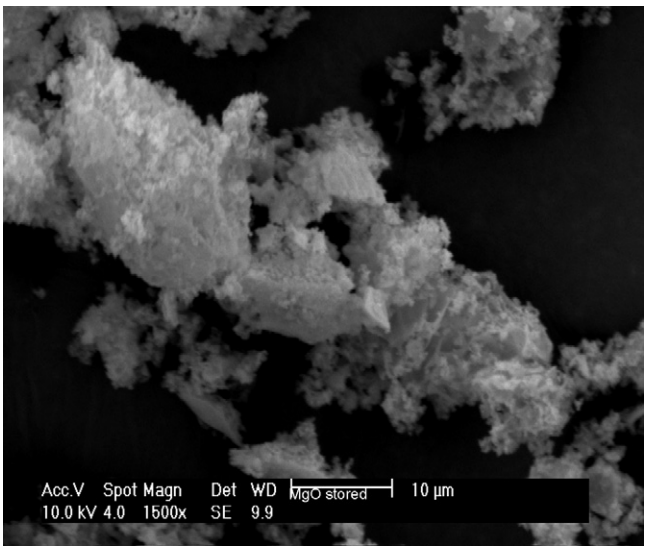

Fig. 5. Scanning electron microscopy (SEM) image for the MgO(stored).

TG-MS coupling analyses of MgO and MgO(C) are presented in Figs. 6–8. Fig. 6 represents the catalysts weight loss, while Figs. 7 and 8 represent the thermal evolution of CO_2 (m/z = 44) and H_2O (m/z = 18) respectively. Fig. 6 shows two major weight loss, one at 120 °C corresponding to hydration water loss as confirmed in Fig. 8; and another between 300 °C and 400 °C. This last weight loss was better understood thanks to MS analyses. Considering CO_2, we observed a desorption at 380 °C for MgO(C) and MgO (Fig. 7). We also observed H_2O desorption peaks at the same temperature that for CO_2 for all the solids (Fig. 8). This desorption of both CO_2 and H_2O at the same temperature proves that the nature of the basic sites are hydrogenocarbonates. The bigger H_2O desorption peak of MgO corresponds to hydroxyl groups. At higher temperature, MgO(C) exhibits two other CO_2 desorption peaks; one at 450 °C corresponding to moderate basic site and another at higher temperature (600 °C) corresponding to strong basic sites. These two last CO_2 desorptions occurs without loss of water, indicating that the nature of the adsorbed sites is carbonates. None of these "chitosan MgO" exhibit carbonate type adsorption sites, but only hydrogenocarbonate ones, which is really unusual for MgO type catalysts. These "chitosan MgO" are then interesting to perform reactions that need moderate basicity as the transesterification reaction. Moreover, the absence of strong basic sites could prevent some side reactions and then the formation of by-products.

3.2. Catalytic testing

The preliminaries results obtained from the catalytic tests (%FAEEs) are shown in Table 1. It can be observed that the materials are active, forming FAEEs with percentages of 30–75% for the fresh catalysts, at 3 h of reaction.

The catalytic activity exhibited by this type of oxide is related to the presence of basic Brøsnted sites in the surface of the material [28,29]. These sites on the magnesium oxide are strong enough, p*Ka* is around 16, to generate alcohoxides which are the active species on transesterification under basic reaction conditions [30,31].

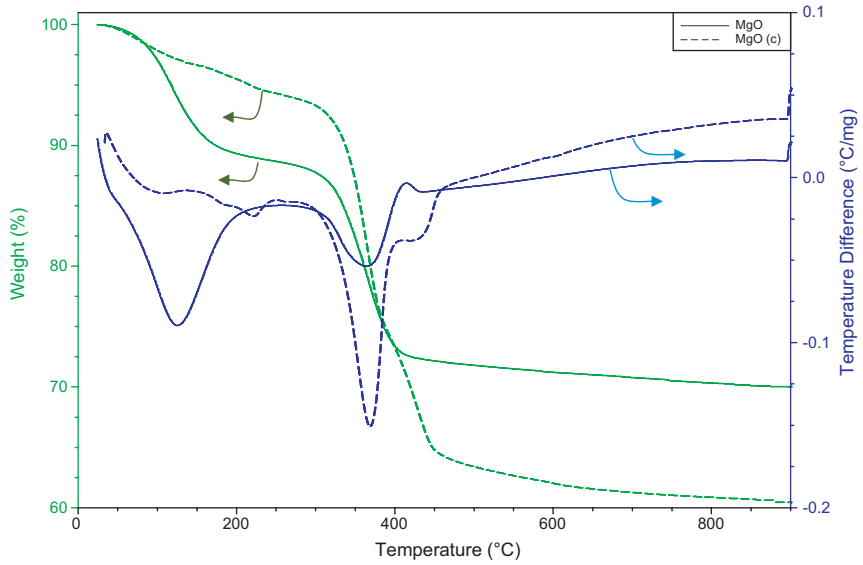

Fig. 6. TG-DTA analysis of MgO and MgO(C).

This study revealed good correlations between the presence of basic sites in the catalysts, as shown in Fig. 7, with the exception of the MgO(stored) sample used to verify the effect of storage in ambient air. The catalyst MgO(stored) was stored in ambient air for a period of 180 days which led to a decrease in the catalyst activity because of the poisoning of the sample by carbonation/hydration of the active sites [15]. The yield of FAEEs decreased from 75% to 14% for the fresh and stored catalysts, respectively.

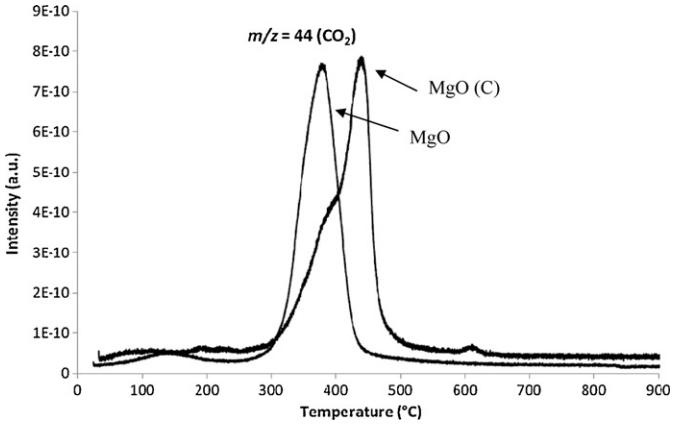

Fig. 7. $m/z = 44$ (CO_2) TG-MS analysis of MgO and MgO(C).

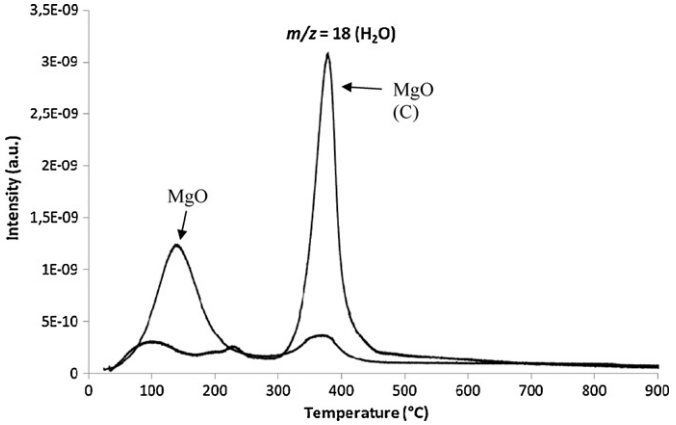

Fig. 8. $m/z = 18$ (H_2O) TG-MS analysis of MgO and MgO(C).

A study on the specific adsorption of CO_2, $CO_2 + H_2O$ as performed to better understand the nature of the poisoning of the catalytic sites (Figs. 9 and 10). When a freshly calcined MgO was analysed by TG-MS, no desorption of H_2O or CO_2 were observed, except a low physisorbed water peak under 100 °C which is due to experimental artifact (refreshment of the oven by undried air). When a freshly calcined MgO was exposed to CO_2 during 15 h, no CO_2 adsorption was detected while when both CO_2 and H_2O were simultaneously put in contact with the same freshly calcined MgO during only 3 h, both of them were adsorbed. If the MgO stays under ambient air more than 2 month after its calcination, the same adsorption is observed with more intensity. It proves that the poisoning of the catalyst is due to the formation of hydrogenocarbonates on the basic catalytic sites of MgO. Only the basic sites corresponding to hydrogenocarbonates adsorption are then involved in the catalytic transeterification of soybean oil by ethanol. We can thus suggest that the storage of the catalyst under dry air could be sufficient to avoid its poisoning. These results are consistent with the characteristics of the MgO catalyst, which has basics sites, this being a requirement for the reaction. In this regard, Henriques and co-workers [8] also showed that MgO, as well as mixed oxides, are efficient catalysts for the transesterification of vegetable oils, using methanol as an alcoholysis agent. They reported a fatty acid methyl ester yield of over 60% at 130 °C for 7 h reaction time. The use of the conventional microcrystalline MgO catalyst in the methylic transesterification of sunflower oil reportedly led to a conversion of 80% at 220 °C [1].

It is important to remark that the catalytic activity is higher for MgO, since CO_2 poisoning is slower over MgO in comparison with MgO(C). In the MgO(C) strong basic Lewis sites are presented and the atmospheric CO_2 reacts very quickly to form less reactive carbonated species. In the case of MgO, the atmospheric CO_2 reacts slowly with moderate Brönsted sites presented, to generate hydrogenocarbonates in the presence of water traces. This is confirmed by the storage study, discussed above.

It is worth noting that along with the ethylic alcohol used in the reaction being of renewable origin, the catalyst was synthesized from chitosan, which is a biomaterial.

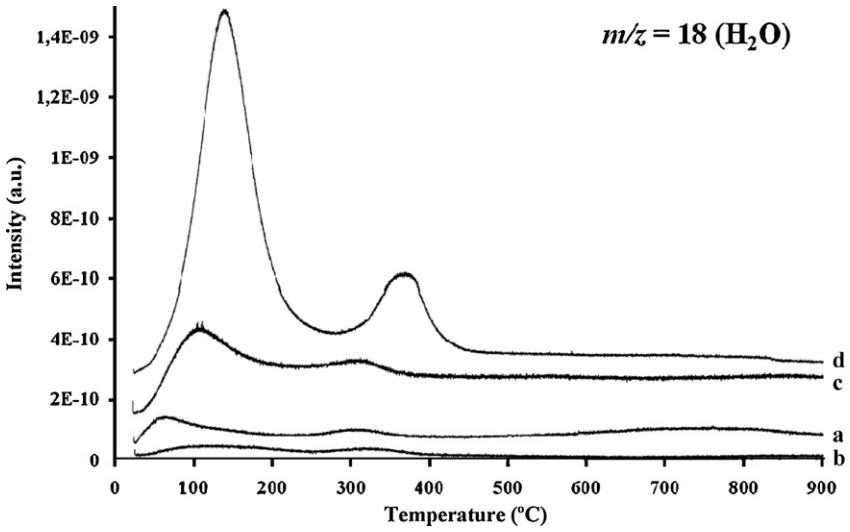

Fig. 9. $m/z = 18$ (H_2O) TG-MS analysis of "chitosan MgO". (a) Directly after calcinations of the precursor, (b) directly after calcinations of the precursor then adsorption of CO_2 during 15 h at 30 °C, (c) directly after calcinations of the precursor then adsorption of both CO_2 and H_2O during 3 h at 30 °C, (d) 2 month of storage after calcinations (MgO(stored)).

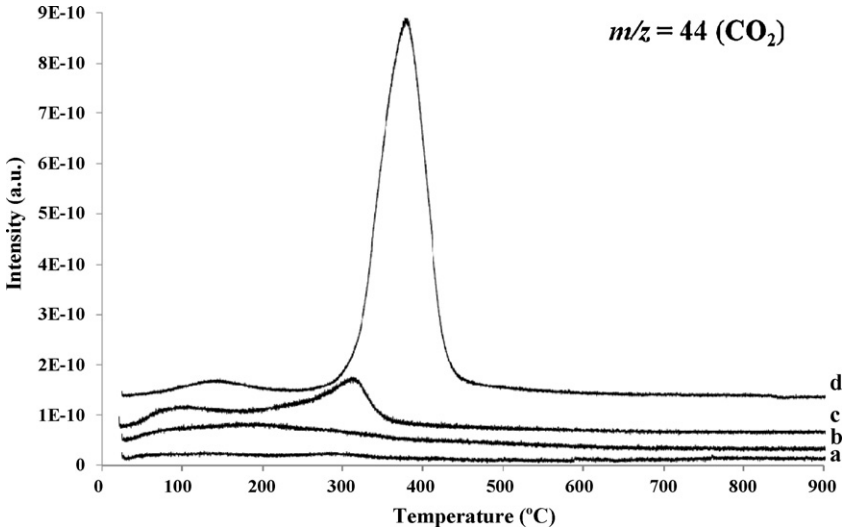

Fig. 10. $m/z = 44$ (CO_2) TG-MS analysis of "chitosan MgO". (a) Directly after calcinations of the precursor, (b) directly after calcinations of the precursor then adsorption of CO_2 during 15 h at 30 °C, (c) directly after calcinations of the precursor then adsorption of both CO_2 and H_2O during 3 h at 30 °C, (d) 2 month of storage after calcinations (MgO(stored)).

4. Conclusions

The method described herein for the preparation of the MgO catalysts via metal–chitosan complexation, led to a significant increase in their surface area and the basicity. These characteristics provide a relatively higher conversion to fatty acid ethyl esters when compared with a commercial oxide. However, solid base catalysts are susceptible to be poisoned by some components in air such as CO_2 and H_2O as they can interact with base sites and decrease catalyst activity.

In this study, higher conversions for the fresh catalysts were associated with lower temperatures and shorter reaction times than those normally found in the literature. This indicates the great potential for the development of heterogeneous catalysts for the production of ethylic biodiesel, allowing conversions equivalent to those obtained with homogeneous catalysts to be achieved under viable reaction conditions from a commercial point of view.

We also proved that both CO_2 and H_2O are necessary to poison the catalyst. Therefore, catalyst activation or proper storage is necessary to maintain catalyst activity and such studies are underway in our research group. This study opens a new approach, employing heterogeneous base MgO catalysts for biodiesel production using ethanol as the alcoholysis agent.

When magnesium oxide is employed for transesterificaion of vegetable oil with ethanol, it is possible that leaching of solid base catalyst occurs. The amount of leached magnesium coming from the catalyst prepared using the metal–chitosan complexation method reached 0.18% during the biodiesel formation.

Acknowledgements

The authors gratefully acknowledge CNPq and FAPEMIG for financial support.

References

[1] M. Verziu, B. Cojocaru, J. Hu, R. Richards, C. Ciuculescu, P. Filip, V.I. Parvulescu, Green Chem. 10 (2008) 373–381.

[2] M.A. Aramendia, V. Borau, C. Jiménez, J.M. Marinas, J.R. Ruiz, F.J. Urbano, Appl. Catal. A: Gen. 244 (2003) 207–215.
[3] S. Bancquart, C. Vanhove, Y. Pouilloux, J. Barrault, Appl. Catal. A: Gen. 218 (2001) 1–11.
[4] D. Gulková, O. Šolcová, M. Zdražil, Microporous Mesoporous Mater. 76 (2004) 137–149.
[5] B.Q. Xu, J.M. Wei, H.Y. Wang, K.Q. Sun, Q.M. Zhu, Catal. Today 68 (2001) 217–225.
[6] V.K. Díez, C.R. Apesteguía, J.I. Di Cosimo, J. Catal. 240 (2006) 235–244.
[7] L. Wang, J. Yang, Fuel 86 (2007) 328–333.
[8] W.M. Antunes, C.O. Veloso, C.A. Henriques, Catal. Today 133 (2008) 548–554.
[9] H.J. Kim, B.S. Kang, M.J. King, Y.M. Park, D.K. Kim, J.S. Lee, K.Y. Lee, Catal. Today 93 (2004) 315–320.
[10] A.A. Kiss, A.C. Dimian, G. Rothenberg, Energy Fuels 22 (2008) 598–604.
[11] X. Liu, H. He, Y. Wang, S. Zhu, Catal. Commun. 8 (2007) 1107–1111.
[12] R.M. Almeida, L.K. Noda, N.S. Gonçalves, S.M.P. Meneghetti, M.R. Meneghetti, Appl. Catal. A: Gen. 347 (2008) 100–105.
[13] H. Hattori, Chem. Rev. 95 (1995) 537–558.
[14] M.L. Granados, M.D.Z. Poves, D.M. Alonso, R. Mariscal, F.C. Galisteo, R. Moreno-Tost, J. Santamaría, J.L.G. Fierro, Appl. Catal. B: Environ. 73 (2007) 317–326.
[15] S. Yan, M. Kim, S.O. Salley, K.Y. Simon Ng, Appl. Catal. A: Gen. 360 (2009) 163–170.
[16] A.C. Pinto, L.L.N. Guarieiro, M.J.C. Rezende, N.M. Ribeiro, E.A. Torres, W.A. Lopes, P.A.P. Pereira, J.B. Andrade, J. Braz. Chem. Soc. 16 (2005) 1313–1330.
[17] H.V. Fajardo, L.F.D. Probst, Appl. Catal. A: Gen. 306 (2006) 134–141.
[18] N.L.V. Carreno, I.T.S. Garcia, C.W. Raubach, M. Krolow, C.C.G. Santos, L.F.D. Probst, H.V. Fajardo, J. Power Sources 188 (2009) 527–531.
[19] J.R.D. Lima, R.B. da Silva, C.C.M. da Silva, L.S.S. dos Santos, J.R. dos Santos, E.M. Moura, C.V.R. de Moura, Quim. Nova 30 (2007) 600–603.
[20] U. Schuchardt, R. Sercheli, R.M. Vargas, J. Braz. Chem. Soc. 9 (1998) 199–210.
[21] A.C. Larson, R.B. Von Dreele, General Structure Analysis System (GSAS), Los Alamos National Laboratory Report LAUR, USA, 2004, pp. 86–748.
[22] B.H. Toby, J. Appl. Cryst. 34 (2001) 210–213.
[23] Inorganic Crystal Structure Database (ICSD), Gmelin-Institut f¨ur Anorganische Chemie and Fachinformationszentrum, FIZ, Karlsruhe, 2007.
[24] A.O. Martins, E.L. da Silva, E. Carasek, N.S. Gonçalves, M.C.M. Laranjeira, V.T. de Fávere, Anal. Chim. Acta 521 (2004) 157–162.
[25] T.C. Coelho, R. Laus, A.S. Mangrich, V.T. de Fávere, M.C.M. Laranjeira, React. Funct. Polym. 67 (2007) 468–475.
[26] B. Song, W. Zhang, R. Peng, J. Huang, T. Nie, Y. Li, Q. Jiang, R. Gao, Colloids Surf. B 70 (2009) 181–186.
[27] H.V. Fajardo, A.O. Martins, R.M. de Almeida, L.K. Noda, L.F.D. Probst, N.L.V. Carreno, A. Valentini, Mater. Lett. 59 (2005) 3963–3967.
[28] D. Gulková, O. Solcová, M. Zdrazil, Microporous Mesoporous Mater. 76 (2004) 137–149.
[29] B.C. Gates, Catalytic Chemistry, First Ed., John Wiley & Sons, New York, 1992.
[30] W.T. Reichle, J. Catal. 94 (1985) 547–557.
[31] M.J. Climent, A. Corma, S. Iborra, J. Primo, J. Catal. 151 (1995) 60–66.